Convective Coupling and Interannual and Intraseasonal Coupled Variabilities in the Tropics

P. GOSWAMI AND RAMESHAN K.

CSIR Centre for Mathematical Modelling and Computer Simulation, Bangalore, India

(Manuscript received 7 August 1996, in final form 30 August 1999)

ABSTRACT

Recent analyses point at close structural similarities and intimate dynamical connections among the members of a wide spectrum of variabilities in the global Tropics. This suggests that these oscillations with widely different timescales may have a common dynamical origin, although diverse dynamical evolution. The present work explores such a dynamical framework for the genesis of tropical variabilities. The highlight of the dynamical framework is a parameterization of air–sea interaction, which the authors call convective coupling. In the proposed parameterization the effect of sea surface temperature (SST) on the atmosphere is only through the modulation of the column precipitation. The changed convective heating modifies the low-level flow, which in turn changes the oceanic variables, thus closing the cycle. Thus the forcing due to convective coupling behaves like a (second order) threshold process, with (SST modulated) convection acting like a switch.

Since many of the observed variabilities exhibit a primarily Kelvin wave structure, the implications of convective coupling are investigated for the dynamics of Kelvin waves. To account for the different mean conditions over which the variabilities of different scales occur, two scenarios, characterized by the strengths of certain physical parameters, are considered to represent the interannual and intraseasonal (mean) conditions. Oscillations of appropriate periods appear for each scenario. Two different representations of dynamics of SST are also considered to explore coupled variabilities in ocean basins with different SST dynamics. It is also shown that the convective coupling can support interannual variability in ocean basins with small zonal scale.

The dynamical scenario that emerges from this study is that the genesis of a wide spectrum of tropical variabilities is caused by a selective excitation of a convectively coupled Kelvin wave embedded in the time-mean state of the corresponding timescale of oscillation. The postgenesis evolution and structure of each oscillation is then influenced by local spatiotemporal characteristics. The results provide both insight for modeling air–sea interaction in the Tropics and constraints for model diagnostics and evaluation.

1. Introduction

It is becoming increasingly evident that the instances of wide spectrum of tropical variability are not dynamically isolated events; they seem to be the members of an organized temporal hierarchy. One indication of this is the close structural similarities among many tropical variabilities. Besides many of these oscillations appear to be dynamically related. Several studies have emphasized the marked similarities between the 30–40-day intraseasonal oscillation (ISO) and the El Niño–Southern Oscillation (ENSO; Madden and Julian 1971; Lau and Chan 1985; Lau and Lau 1986; Barnett 1984). The close relationship between the ENSO and the annual and the seasonal cycles has also been emphasized. The strong interrelation between ENSO, quasi-biennial oscillation and the annual cycle has been also pointed out by Rasmusson et al. (1990). It is tempting to think that many of these variabilities originate from a common dynamical mechanism, although the postgenesis evolution and structure of each variability may be more diverse owing to secondary dynamical processes that depend on local conditions and parameters. Identification of such a common mechanism of genesis will provide, in addition to enhancing our understanding of the complex dynamics of tropical atmosphere, valuable aid for improving model simulation and forecast at various scales.

While the choice of such a primary dynamical mechanism(s) for genesis is not a priori obvious, it is clear that the mechanism must be one that is operative over a wide spectrum of timescales. The most promising candidate seems to be ocean–atmosphere coupling (OAC) as many of these variabilities are now found to be present both in the atmosphere and the ocean. Recent analyses reveal that ocean–atmosphere coupling plays a significant role in a wide spectrum of oceanic and atmospheric variabilities in the Tropics. Following the conceptualization by Bjerknes (1969), it has long been held

Corresponding author address: Dr. P. Goswami, CSIR Centre for Mathematical Modelling and Computer Simulation, Bangalore 560 037, India.
E-mail: goswami@cmmacs@ernet.in

that ENSO is an ocean–atmosphere coupled instability. Importance of OAC in the annual cycle has been shown for the eastern Pacific and the Atlantic Oceans by observational studies of Mitchell and Wallace (1992) and Wang (1994). Wang (1994) used monthly SST fields for the period 1950–87 obtained from the Comprehensive Ocean–Atmosphere Data Set to investigate the annual cycle in the tropical Pacific (between 30°S–30°N and 120°E–76°W). His analysis reveals two distinct components of variations in SST with respect to the equator. One antisymmetric, extratropical component that explains about 70% of the SST variance on the average and a symmetric equatorial annual cycle (SEAC). The SEAC is found to dominate the central-eastern equatorial Pacific, with amplitude decreasing with distance away from the equator. Wang (1994) concludes that while the antisymmetric component is essentially a delayed response to solar radiation with a maximum in the late summer (minimum in the late winter), the SEAC is primarily governed by OAC, with maximum (mininum) in late fall (spring). In an earlier study Wang (1993) demonstrated the important role played by OAC in the annual development of the cold tongue in the eastern Pacific. Covering the range from decadal to interannual to seasonal, the tropical ocean–atmosphere also exhibits strong signals at intraseasonal timescales (IST). The best known example of atmospheric ISO is the 40–60-day Madden–Julian oscillation (Madden and Julian 1971, 1972). It is now known that a prominent intraseasonal signal is present also in the oceanic circulation. Although in the intraseasonal scale the role of OAC has been less clear, recent analyses of outgoing longwave radiation data (January 1985–April 1991) from International Satellite Cloud Climatology Project (ISCCP) as well as European Centre for Medium-Range Weather Forecasts surface analyses (January 1985–December 1994) indicate strong interaction between ocean and atmosphere at IST (Jones et al. 1996). Other studies (Shinoda et al. 1998) using independent datasets also confirm ocean–atmosphere interaction at ISO timescales. The mechanism of OAC, therefore, appears to be operative over a wide spectrum of tropical variabilities.

a. The principle of convective ocean–atmosphere coupling (COAC)

Most of the attempts to develop a dynamical mechanism to explain the coupled variabilities in the Tropics, however, have focused on the ENSO. The basic premise of many of these studies is that while the linear atmosphere and the ocean may be by themselves stable, OAC can make the (coupled) system unstable. The OAC in these studies involves a mechanical coupling that determines a forcing of the oceanic current by the (lower) atmospheric wind stress and a thermal coupling that determines the effect of SST on atmospheric heating. In most of the studies mentioned above, the latter is prescribed as a proportionality relation between SST anomaly and perturbation heating of the atmosphere. In such a formalism, SST acts like a direct heat source for the atmosphere, and the link between SST and atmospheric convection is an implicit one. Of course, the direct heat source provided by SST implicitly involves the convective processes, in the sense that the changed low-level circulation will result in modified intensity and distribution of convection. Although there have been a few attempts to incorporate the effects of convection directly into the formulation of OAC (Lau and Shen 1988; Goswami and Selvarajan 1991), these formulations can be termed as direct coupling where SST can heat the (lower) atmosphere, regardless of presence or absence of convection. The role of convection in these formulations is indirect or implicit. One reason for the indirect role of convection in these studies is that the moisture variable, and hence the precipitative heating, is determined by a balance equation. It should be noted that although Lau and Shen (1988, hereafter LS) begin with a dynamic moisture equation, their subsequent assumption of a convective regime effectively removes the time dependence of the moisture variable. However, in a dynamical scenario the convective and nonconvective regimes themselves evolve, one changing to the other depending on the local and time-dependent forcing of the moisture variable. This is particularly true for a coupled environment, where SST plays a crucial role in the moisture variable. Indeed, recent analyses seem to indicate that the atmospheric convective activity is inseparably coupled to the oceanic processes. Several studies point to strong association between SST and the atmospheric convective activity at different timescales. In an analysis of data from ISCCP, Weare (1994) found significant correlation of SST with cloud variables both at IST and interannual timescales (IAT). Weare further shows that not only SST but time rate of change of SST is also important for these processes. From a study of intraseasonal variability of the tropical Pacific–Indian Ocean and atmosphere using 7-yr (1986–93) daily gridded data for OLR, surface stress, and SST, Hendon and Glick (1995) report on the significant role of intraseasonal (30–50 day) cloud activity, and resultant shortwave anomalies, on SST, especially over the Indian Ocean eastward of about 165°E. The importance of the evaporative process in ENSO-type interannual variability (ETIAV, variabilities with periods between 3 and 4 yr) has been emphasized by Mayers et al. (1986).

The above analyses thus point to the possibility that the mechanism of OAC, in general, may involve SST in a way different from the one usually assumed. While a strong association between SST and (low level) convection is quite expected, the observed association between SST and cloud activity, in particular, shows that the entire (lower) atmospheric column and the convective activity are directly involved in OAC. It is possible that the primary mechanism of OAC is through the ef-

fect of SST on the atmospheric convection. This would imply that, unlike in the conventional formalism where the atmospheric heating is directly controlled by SST, the (OAC induced) atmospheric heating is possible only through deep heating by the column precipitation. In particular, in such a scenario, OAC behaves like a (second order) threshold process, somewhat akin to first-order phase transition that results in precipitation. In the same way that precipitation cannot occur until the moisture content exceeds a critical value, the OAC induced atmospheric heating in our scenario is not effective until SST induced convection reaches a critical value. We shall call such a representation of OAC convective coupling, to contrast it from the conventional (direct) coupling. Thus, if the basic mechanism of direct coupling can be summarized as the circular interaction between (low level) winds affecting the ocean, which in turn affects the winds, then the basic mechanism of convective coupling can be represented as convective forcing affecting the winds, which affect the ocean, which in turn affect the winds and convective forcing.

b. The choice of the dynamical system

The purpose of this study is to formulate such a convective coupling and to explore the dynamics of a convectively coupled system. A noteworthy feature of many of the observed variabilities in the Tropics is their predominantly Kelvin wave character. The central role played by the Kelvin waves in ENSO has been emphasized and utilized in many studies (Hirst 1988; Hirst and Lau 1990; Philander 1990). Similarly, the prominent atmospheric ISO with 40–60-day scale is also known to exhibit a prominent Kelvin wave character (Madden and Julian 1971; Lau and Chan 1985; Knutson and Weickman 1987; Weickman et al. 1985). Importance of the Kelvin waves in the dynamics of oceanic ISO has been also well recognized (Johnson and McPhaden 1993; Hendon and Glick 1995). Analysis of time series data from surface moored buoys in the Eastern equatorial Pacific (110°–140°W) for the period 1975–83 by McPhaden and Taft (1988, hereafter MT) revealed a very prominent ISO in zonal current, temperature, and dynamic height. In the analyses of MT the signals were found to have characteristics of Kelvin waves, with eastward propagation, zero meridional velocity, and with zonal velocity and temperature nearly in phase. Enfield (1987, hereafter E87) showed that the sea level fluctuations at IST during 1975–84 along the west coast of the Americas are remotely forced by atmospheric ISO in the western Pacific. These forced signals with Kelvin wave structure propagate eastward across the equator to reach the eastern boundary, where they propagate as coastal Kelvin waves. Although the analysis of MT revealed the period of the signals to be 60–90 days as against 40–60 days found by E87, it is likely that both the signals represent the same physical process (MT). A scenario that provides a qualitative understanding for such a situation is discussed later using the present model. All these studies indicate that Kelvin wave dynamics plays a central role in the tropical variabilities at IST, IAT as well as at intermediate timescales. We shall therefore consider convectively coupled Kelvin waves to explore a unified dynamical mechanism for origin of coupled oscillations at different timescales.

While we confine our dynamics to Kelvin waves, we address several questions pertaining to coupled variabilities in the Tropics. In particular, it is shown that the convectively coupled system can support a wide spectrum of oscillations characterized by the selectively destabilized waves (the mode with the largest growth rate in the lower frequency regime; hereafter SDW) with different periods and wavelengths. Thus the two prominent oscillations, namely ENSO and ISO, with two widely different timesscales appear as manifestations of a single dynamical mechanism. However, such a unified dynamical framework for oscillations, with periods ranging from IST to IAT, must take into account the differences in the strengths and the relative roles of various processes at the widely separated timescales. Thus we consider two scenarios: one representative of IST and the other representative of IAT. These scenarios, as described below, are characterized by the strengths of certain physical processes appropriate for the respective timescale. In addition we also consider scenarios that are region specific, such as the Indian Ocean summer monsoon region. It will be seen that the same mechanism that gives rise to interannual oscillation (IAO) generates ISO as one changes from the IAT to IST scenario. For intermediate scenarios the mechanism can generate oscillations of seasonal and annual timescales.

Another important question we address is the global nature of ETIAV. In particular, recent analysis reveals that ETIAV is a phenomenon present over the global Tropics (Yasunari 1987; Nigam and Shen 1993; Tourre and White 1995). Thus, ETIAV, almost in phase with the Pacific events, but with lower amplitudes, also appear over the equatorial Indian Ocean. In addition, interannual signals are also observed over the Atlantic Ocean (Zebiak 1993). It is possible that both regional mean conditions as well as basin-specific SST dynamics contribute to the genesis of IAO with relatively short zonal scale. We therefore consider two ocean models, characterized by different dynamics of SST. We then explore whether either of the SST models can support interannual variabilities with relatively shorter zonal scale.

In section 2 we describe the two components (atmospheric and the oceanic) of our basic model, the concept and formulation of the convective coupling, and the two scenarios. Section 3 discusses the dispersion relation and the eigenfunctions for the two ocean models. In section 4 we discuss the mechanisms of ISO and IAO in the two ocean models and the relative roles of various processes. Section 5 presents our conclusions.

2. The basic model

a. The atmospheric component

Since in our scenario, the entire lower atmosphere is affected by OAC, we consider an atmospheric component of the coupled model that describes the dynamics of anomaly circulation of the lower troposphere. This component is represented by the shallow water equations describing the horizontal structure of the first baroclinic mode on an equatorial β plane. This system has been used in several studies (Davey 1985; LS; Davey and Gill 1987; Goswami and Goswami 1991). Because of the first baroclinic mode vertical structure used in these models, they are equivalent to models of the lower troposphere. Conventionally this system includes three equations describing the evolution of perturbations of zonal and meridional wind components (u and v, respectively) at the lower layer and the midlevel potential temperature perturbation θ. In the present study we also have a fourth equation describing the evolution of the positive moisture anomaly over an equilibrium value $\overline{q}$ of depth-integrated moisture (Goswami and Rao 1994, hereafter GR). For the Kelvin wave, the nondimensional forms of these equations are given by

$$\frac{\partial u_a}{\partial t} - \frac{\partial \theta}{\partial x} + Ru_a = 0, \tag{1}$$

$$\beta y u_a - \frac{\partial \theta}{\partial y} = 0, \tag{2}$$

$$\frac{\partial \theta}{\partial t} - \frac{\partial u_a}{\partial x} + R\theta = Q, \tag{3}$$

$$\frac{\partial s}{\partial t} + \Gamma \frac{\partial u_a}{\partial x} = E - P, \tag{4}$$

$$q = \overline{q}(1 + s). \tag{5a}$$

The subscript a denotes atmospheric variables. Here, R represents both Rayleigh damping and Newtonian cooling coefficients, which we consider to be equal as their difference was not found to change the results qualitatively.

The evolution of the moisture variable s (expressed as a fraction of some reference value $\overline{q}$), is described by Eq. (4), with the right-hand side describing source and sink of the moisture variable. Here E is the gain due to evaporation from the surface and P is the loss due to precipitation in the column. The moisture scale for nondimensionalizing this equation has been taken as $\overline{q}$ ($\approx$50 kg m^{-2}). Here

$$\Gamma = -\frac{H}{\overline{q}} \int_0^{H_o} \frac{dq^*}{dz} f(z)\, dz. \tag{5b}$$

In the above expression, H_o represents a height relevant for moisture dynamics and the unit of q^* is kg m^{-3} and $f(z)$ is a nondimensional structure function representing the vertical structure of the dynamical fields. Since our model is one for the first baroclinic structure, we consider $H_o = H$. We assume, for simplicity, that dq^*/dz is independent of height and its value is estimated by assuming $q^*(H) = 0$, and a climatological value for $q^*(z = 0)$. The value of latter, and hence the value of Γ, depends on the scenario (IST, IAT, etc.). It should be noted that the explicit time dependence of the moisture variable in our study allows us to avoid assuming a permanently convective region assumed in many studies (e.g., LS; Goswami and Goswami 1991). In our formalism a nonconvective (convective) region can evolve to a convective (nonconvective) region through the evolution of the moisture variable.

The precipitation brings the moisture variable q to its equilibrium value $\overline{q}$ over a timescale τ; thus in its dimensional form

$$P = \frac{q - \overline{q}}{\tau} = \frac{s\overline{q}}{\tau}. \tag{6}$$

In other words the moisture variable does not relax back to its equilibrium value $\overline{q}$ immediately but does so over a moisture relaxation timescale τ. Several studies have emphasized the role and importance of a convective time lag in tropical circulation (Betts 1986; Betts and Miller 1986; Emanuel 1993; Goswami and Roa 1994; Goswami and Mathew 1994; Neelin and Yu 1994). The concept and the effect of a moisture relaxation timescale were discussed in detail in GR. The basic philosophy is that for organized large-scale precipitation in the Tropics, the process cannot be considered instantaneous; it has a characteristic relaxation timescale that can be typically a few hours. Recently Seager and Zebiak (1995) have also used a time lag of a few hours, although in a different context.

In the present work, as in GR, we shall assume a convective time lag (CTL) between organized convection and large-scale response to be a few hours. It should be noted that the CTL embodies our hypothesis and it is not possible to assign a precise value to it at present. However, we shall assume that the CTL timescale corresponds to the timescale of mesoscale organization, that is, a few hours. It will be seen, subsequently, that once the concept of a CTL is incorporated, the results are not very sensitive to its specific value, except for extreme values.

The length, time, and temperature scales used for nondimensionalizing our equations are given by

$$T_0^2 = \frac{1}{2\beta_d c_a}\frac{\overline{\theta}}{\theta_0}, \qquad L_0^2 = \frac{c_a}{2\beta_d}\frac{\overline{\theta}}{\theta_0}, \qquad \theta_0 = H\frac{d\overline{\theta}}{dz} \quad \text{and}$$

$$c_a^2 = \frac{gH\theta_0}{\overline{\theta}}.$$

The values of these quantities are given in Table 1a. The perturbation evaporation E is controlled by both atmospheric and oceanic processes. While a high SST enhances potential evaporation, ventilation by the sur-

TABLE 1a. Description of the model parameters.

Parameter	Dimensional		Nondimensional	
	Symbol	Value	Symbol	Value
Timescale	T_o	0.85 day	—	—
Length scale	L_o	4400 km	—	—
Temperature scale	θ_o	21 K	—	—
Moisture scale	q_o	40–50 kg m^{-2}	—	—
Mean potential temperature	$\bar{\theta}$	310 K	—	—
Mean thermoline depth	$\bar{h}$	70 m	—	—
Oceanic gravity wave speed	c_o	1 m s^{-1}	—	—
Tropopause height	$H\pi$	16 km	—	—
Atmospheric dry gravity wave speed	c_a	200 m s^{-1}	—	—
Convective time lag	τ	0.25 day	B	3.4
Upwelling coefficient	δ_d	0.02 K m^{-1}	δ	9×10^{-4}
Oceanic Rayleigh friction coefficient	a_d	80 day^{-1}	a	10^{-2}
Oceanic Newtonian cooling coefficient (for ϕ and T)	b_d	200 day^{-1}	b	4.3×10^{-2}
Atmospheric Rayleigh friction coefficient	R_d	1–5 day^{-1}	R	0.17–0.85
Atmospheric Newtonian cooling coefficient	R_d	1–5 day^{-1}	R	0.17–0.85

face wind is necessary to make the evaporation process effective. The contribution from the atmospheric process to evaporation comes essentially from evaporation–wind feedback (EWF). If we assume these two processes to work in an additive manner (LS), then we can write

$$E = \alpha T + \Lambda u_a, \tag{7}$$

where the nondimensional forms for the evaporation–SST feedback parameter α and EWF parameter Λ are given in the following:

$$\alpha = \frac{\alpha_d \theta_0 T_0}{\overline{q}} \quad \text{and} \quad \Lambda = \frac{\rho_a C_D \Delta q L_0}{\overline{q}}.$$

The various symbols with subscript *d* used in this paper denote the corresponding dimensional value of the parameters represented by the symbols. The sign of Λ(as given in Table 1) can be either positive or negative depending on whether the mean background winds are (implicitly) assumed to be westerlies or easterlies (Neelin et al. 1987). Although the mean background winds in the Tropics are easterlies in general, there are situations (e.g., Indian Ocean summer monsoon) when the mean winds are westerlies. Thus we shall consider either of the signs of Λ depending upon the situation. The values of Δq used are adopted from earlier studies (Weare et al. 1981; Zhang and McPhaden 1995).

As in GR, the atmospheric heating is considered proportional to precipitation, which in turn is proportional to *s*, as can be seen from Eq. (6). Thus the nondimensional form of heating is given by

$$Q = \eta s; \tag{8}$$

where $\eta = (L_v B\overline{q})/(\theta_0 C_p H \rho_a)$. The constants L_v, C_p, ρ_a, and H are described in Table 1. The nondimensional form of the other parameters in the model equations are $R = R_d T_0$, $B = T_0 \tau^{-1}$, and $\beta = \beta_d L_0 T_0$.

b. The oceanic component

The basic ocean model describes the dynamics of an oceanic mixed layer using reduced gravity equations for Kelvin waves. In addition we consider two equations that represent dynamics of SST in different ocean basins or in different situations.

SST-model I:

In the Eastern Pacific, for example, there exists an observed positive correlation the thermocline depth *h*

TABLE 1b. Description of the coupling and scenario parameters. SST-M1 stands for SST-model I and SST-M2 stands for SST-model II.

Parameter	Symbol	Nondimensional value			
		Intraseasonal		Interannual	
		SST-M1	SST-M2	SST-M1	SST-M2
Evaporation–wind feedback	Λ (10^{-1})	5.0	−1.0	2.5	2.5
Convergence feedback	Γ	1.35	1.2	1.2	1.0
Zonal gradient of mean SST	G (10^{-2})	−10.5	12.5	−8.5	−7.5
Wind–SST feedback	α	4.6	4.6	4.6	4.6
Coefficient of mechanical coupling	γ (10^{-3})	9.5	9.5	9.5	9.5

and SST (Philander et al. 1984). Therefore, in our first SST model we take

$$T = \zeta h, \tag{9}$$

where ζ is a constant of proportionality of the order of 10^{-2} K m^{-1}. This is in accordance with the value of ζ used by Hirst (1986). Then the governing equations for model I can be written as

$$\frac{\partial u_o}{\partial t} + \epsilon\frac{\partial T}{\partial x} + au_o = \tau_x, \tag{10}$$

$$\beta y u_o + \epsilon\frac{\partial T}{\partial y} = 0, \tag{11}$$

$$\frac{\partial T}{\partial t} + \zeta^*\frac{\partial u_o}{\partial x} + Gu_o + bT = 0, \tag{12}$$

where $\zeta^* = \zeta\overline{h}/\theta_0$, $\epsilon = \theta_0 g' T_0^2/\zeta L_0^2$, and $G = \zeta L_0/\theta_0(d\overline{h}/dx)$.

SST-model II:

Unlike in the Pacific basin, which has a shallow thermocline, the SST, in general, follows its own dynamics, although it is significantly affected by upwelling and downwelling. Thus in our second model SST is governed by an independent dynamical equation similar to one used in LS:

$$\frac{\partial u_o}{\partial t} + \epsilon\frac{\partial \phi}{\partial x} + au_o = \tau_x, \tag{13}$$

$$\beta y u_o + \epsilon\frac{\partial \phi}{\partial y} = 0, \tag{14}$$

$$\frac{\partial T}{\partial t} + Gu_o + bT = \delta\frac{\partial \phi}{\partial t}, \tag{15}$$

$$\frac{\partial \phi}{\partial t} + \frac{\partial u_o}{\partial x} + d\phi = 0, \tag{16}$$

where $\epsilon = \overline{\phi}T_0^2/L_0^2$, $G = L_0/\theta_0(d\overline{T}/dx)$, $\delta = \overline{\phi}\,\delta_d/\theta_0$, and $\overline{\phi} = c_0^2$.

In Eqs. (10)–(16), a, b, and d represent, respectively, damping coefficients for momentum, SST, and the geopotential in nondimensional form (Table 1b). For convenience, we use the same symbols (ϵ and G) to represent the similar processes in two SST models, though the values and forms of their nondimensional counterpart differ. The variables u_o and T are perturbations in zonal current and SST, respectively. The thermocline height (in geopotential units) of the upper ocean is denoted by ϕ. The parameters appearing in Eqs. (1)–(16) are described in Tables 1a and 1b. It is worthwhile to examine the basic difference between the two SST models. For example, Eq. (15) can be rewritten using Eq. (16) as

$$\frac{\partial T}{\partial t} + \delta\frac{\partial u_o}{\partial x} + Gu_o + \left(b + \frac{d\delta g}{\zeta}\right)T = 0,$$

where the linear dependence of T and h [Eq. (9)] is assumed. Thus the above equation is equivalent to Eq. (12) when the respective coefficients are identified. In this sense SST-model I is more general. However, as Eq. (9) represents a known oceanic condition, it is instructive to consider SST-model I separately

The nature of the ocean–atmosphere coupling depends on the prescribed functional dependence of the wind stress τ and the atmospheric heating Q. For the mechanical coupling through the wind stress, we have adopted the conventional parameterization, $\tau_x = \gamma_d u_a$, where γ_d represents the coefficient of mechanical coupling whose nondimensional form is given by $\gamma = \gamma_d T_o$.

In the convective coupling that we propose, SST cannot heat the atmosphere directly; it influences the atmospheric heating by controlling the column moisture, and hence column precipitation. Further, the atmosphere is driven solely by precipitational heating. As such, the influence of the oceanic variables on the atmospheric flow would be absent in the absence of precipitative process. This process is included through Eqs. (3), (4), and (7).

c. The interannual and the intraseasonal scenarios

One of the prime objectives of our study is to explore a common dynamical mechanism for the genesis of coupled variabilities in the Tropics. However, while the basic dynamical mechanism may be the same, the oscillations with widely different timescales, like IAO and ISO, occur over different mean states. Although there is no explicit reference to a mean flow, we need to incorporate this difference in the mean conditions. One of the effects of the mean conditions is that the strengths and the relative roles of various processes, especially those that depend on the mean conditions, are likely to be quite different for widely separated timescales. For example, selective destabilization of waves at ISO (IAO) scale cannot possibly be expected to occur for parameter strengths that are representative of the IST (IAT). It is therefore important to take this aspect into account. In view of paucity of appropriate data, it is not easy to quantify these changes in the parameters as we change from one timescale to another. We shall, therefore, attempt to identify parameters that can provide a qualitative classification of scenarios with widely different timescales. In particular, we shall choose these parameters so as to be consistent in their characteristics with the respective timescale. Thus, for example, a value of Λ that is relevant for IST should only accompany a value of G relevant for the same timescale. Following this reasoning, we consider two scenarios, namely, interannual and intraseasonal, for the same dynamical system described by the above equations. These two scenarios, for each ocean model, are characterized by parameters that reflect the mean conditions (and hence timescales). In general, quantities averaged over IAT are likely to be smaller than those averaged over IST.

Therefore, we shall assume a value for a scenario parameter for IAT smaller than its corresponding value for IST. Specific reasons for this can vary from parameter to parameter and will be indicated below. Discussion on intermediate timescales can be accommodated by considering parameters of intermediate strengths. We choose the following scenario parameters.

1) STRENGTH OF EWF (Λ)

This parameter is essentially determined by the time-mean value of the air (anemometer level)–sea humidity difference. Following the reasoning outlined above, we assume that the interannual scale is characterized by a value of Λ smaller than that for the IST. This can happen, for example, because the air–sea humidity difference Δq in the IAT contains an average over summer as well as winter conditions, and hence would be smaller than the value averaged over only summer conditions. In addition, for IST, as in the Indian Ocean summer monsoon region, the mean winds can be westerly. Thus for the ISO, both these cases are considered. For the values of mean wind assumed in our model (5 m s^{-1}), the observed value of Δq is about 3 gm kg^{-1} (Zhang and McPhaden 1995), which corresponds to the value of Λ 0.5. We consider this value to characterize our intraseasonal scenario.

2) ZONAL GRADIENT OF MEAN SST (G)

It is well known that zonal gradient of mean SST plays an important role in coupled dynamics (LS). However, the value of G is likely to be different for IAT and IST. In addition the value of G also varies from basin to basin. For example, the summer monsoon Indian Ocean is characterized by a positive east–west SST gradient, while, in the interannual scale, the Pacific is characterized by a negative east–west gradient of SST (Philander 1984)—the one used in many earlier studies (Hirst 1988; Lau and Shen 1988), for the interannual timescale.

3) STRENGTH OF CONVERGENCE FEEDBACK (Γ)

The value of convergence feedback, whose nondimensional strength is measured by Γ, varies from IST and IAT. If we assume the IST to represent the summer situation, the value of Γ for the IAT will be less than that for the IST. For a variation of $q(z = 0)$ from 0.002 to 0.015 gm kg^{-1} Eq. (5b) implies a range of $0.01 < \Gamma < 1.6$. Thus we adopt a value of Γ between 1 and 1.5 with the smaller limits to characterize IAT scenario.

It is possible to name other variables, like the mean thermocline depth ($\overline{h}$), strength of the mean wind, and the mean lapse rate of the atmosphere, that are different for different timescales and for different regions. However, we shall confine ourselves mainly to these three parameters to characterize the scenarios; roles of certain other parameters are discussed in appropriate context. Certain important physical quantities as well as the parameters that do not change with timescale are described in Table 1a, while the standard values of the parameters for the two scenarios are given in Table 1b. The question of sensitivity of the results to these parameters will be taken up subsequently.

3. The dispersion relation and the eigenfunctions

For both the SST models, we seek separable solutions for the coupled systems in the form

$$\xi(x, y, t) = \xi(y)e^{i(kx - wt)}. \tag{17}$$

Here ξ represents any of the variables u_a, v_a, θ, s, u_o, T, and ϕ. The conditions for obtaining nontrivial solutions then result in a dispersion relation for each ocean model.

a. The dispersion relations

SST-model I:

$$i\alpha\gamma\eta kG^* - [\sigma_B(k^2 - \sigma_R^2) - i(\Gamma k - i\Lambda)\eta k](\sigma_a\sigma_b + k\epsilon G^*) = 0, \tag{18}$$

where $G^* = (iG - \zeta^* k)$.

SST-model II:

$$\alpha\gamma\eta k(\delta\omega k - iG\sigma_d) - \sigma_b[i\sigma_B(k^2 - \sigma_R^2) + (\Gamma k - i\Lambda)\eta k](\sigma_a\sigma_d - k^2\epsilon) = 0, \tag{19}$$

where $\sigma_R = \omega + iR$, $\sigma_B = \omega + iB$, $\sigma_a = \omega + ia$, $\sigma_b = \omega + ib$, and $\sigma_d = \omega + id$.

Equations (18) and (19) can be expressed as polynomials in ω of degrees, respectively, 5 and 6. The expressions for these polynomials and the coefficients were arrived at using the MATLAB symbolic processor. The resultant polynomials are solved for various values of k (real). Hence, in general ω is a complex quantity. For further analysis of the dispersion relations we need to look at the structures of the eigenfunctions.

b. The eigenfunctions

Since the form of the equations governing the atmospheric part does not depend on the particular ocean model, the functional forms of the atmospheric variables are also independent of the ocean model. So the eigenfunction of the zonal wind can be written as

$$u_a(x, y, t) = \exp(ikx - i\omega t - \Delta y^2), \tag{20}$$

where

$$\Delta = \frac{\beta k}{2\sigma_R}. \tag{21}$$

As stated earlier, ω is in general complex and hence the meridional structure of the waves are trapped only when $\mathrm{Re}(\Delta) > 0$. The eigenfunctions for the other atmospheric variables are given below in terms of u_a:

$$\theta = -\frac{\sigma_R}{k}u_a, \tag{22}$$

$$s = \frac{i(k^2 - \sigma_R^2)}{\eta k}u_a. \tag{23}$$

c. The oceanic eigenfunctions

SST-model I:

$$u_o = \frac{i\gamma\sigma_b}{\sigma_b\sigma_a + \epsilon kG^*}u_a \tag{24}$$

$$T = -\frac{i\gamma G^*}{\sigma_b\sigma_a + \epsilon kG^*}u_a \tag{25}$$

SST-model II:

$$u_o = \frac{i\gamma\sigma_d}{\sigma_d\sigma_a - k^2\epsilon}u_a, \tag{26}$$

$$T = \frac{i\gamma(\delta\omega k - iG\sigma_d)}{\sigma_b(\sigma_d\sigma_a - k^2\epsilon)}u_a, \tag{27}$$

$$\phi = \frac{i\gamma k}{\sigma_d\sigma_a - k^2\epsilon}u_a. \tag{28}$$

The physical fields are the real parts of these complex functions.

d. General characteristics of the dispersion relation and the eigenfunctions

We have solved the dispersion relations (18) and (19) subject to the consistency condition: $\mathrm{Re}(\Delta) > 0$. Before going into the detailed study of the full dispersion relations, it is instructive to analyze one of its limiting cases: $B = 0$. In our model the parameter B controls the atmospheric heating; thus, $B = 0$ corresponds to a case when precipitational heating is absent. As noted earlier there is no direct contribution of SST to atmospheric heating and SST controls the atmospheric heating only by controlling the moisture availability of the atmospheric column. Thus in absence of precipitational heating ($B = 0$), there is no contribution of the oceanic variables to the atmospheric heating. This is reflected in the dispersion relations by the fact that the terms involving $\alpha\gamma$ disappear for $B = 0$. The same argument also holds for EWF, which can affect the atmospheric heating only through affecting the atmospheric column moisture. Thus for $B = 0$, all the terms involving EWF parameter (Λ) drop out of the dispersion relations. In other words coupling cannot give rise to ocean–atmosphere instability in the absence of precipitational heating.

The other extreme case is represented by $\tau \to 0$, which implies $P \to \infty$, implying an instantaneous relaxation of the moisture field. Although it is possible to analyze the case mathematically, it is not physically relevant as it would introduce unrealistically large precipitational heating for even a small perturbation in the moisture. The singularity at $\tau = 0$ merely reflects the fact that an appropriate limiting case is not $\tau = 0$. In the following we shall, therefore, explore the dispersion relations for the existence of selectively destabilized waves that can correspond to observed variabilities. Although we shall demonstrate that our framework can support a wide spectrum of coupled variabilities, our emphasis is on interannual and intraseasonal oscillations. In particular, we shall look for SDW with appropriate time period and zonal scale for values of the parameters that belong to either of the scenarios.

e. Interannual and intraseasonal oscillations—The standard case

Out of the allowed solutions of the dispersion relation, only the ones that have positive growth rates are physically relevant. The growing solutions of the dispersion relation for the ocean models I and II are accordingly presented in Fig. 1. The top panels represent the intraseasonal scenario while the bottom panels represent the interannual scenario. The left panels show the variation of the real part of ω (frequency) with wavenumber k in nondimensional units. The corresponding variations of the growth rate (imaginary part of ω) are shown in the right panels, for ranges of k and ω appropriate for the two timescales. In each panel the solid line represents the ocean model I while the dashed line represents the ocean model II. Not all the part of the curves are allowed. The circles are used to mark the beginning of the allowed region. The arrow marks on the left panels indicate the wavenumbers corresponding to the maximally growing waves. The various values of the parameters are taken for the standard cases for the corresponding timescale as given in Table 1b. It should be noted that for the SST-model II and for IST, the standard value of EWF corresponds to mean westerlies, which is more appropriate for the situation over the Indian Ocean.

The time periods and wavelengths for each scenario and for each ocean model are given in the respective panel, where the subscripts 1 and 2 refer to ocean model I and II, respectively. It can be seen that for each ocean model and for each scenario there exists SDW at appropriate timescales. Because of the consistency condition [i.e., $\mathrm{Re}(\Delta > 0)$] westward propagating Kelvin waves are not allowed.

The dispersion curves exhibit several interesting features. For example, for both the ocean models and for both the timescales, the dispersion curves resemble the classical dispersion curve for Kelvin wave (with $\omega = ck$) only for some of the solutions and only for short

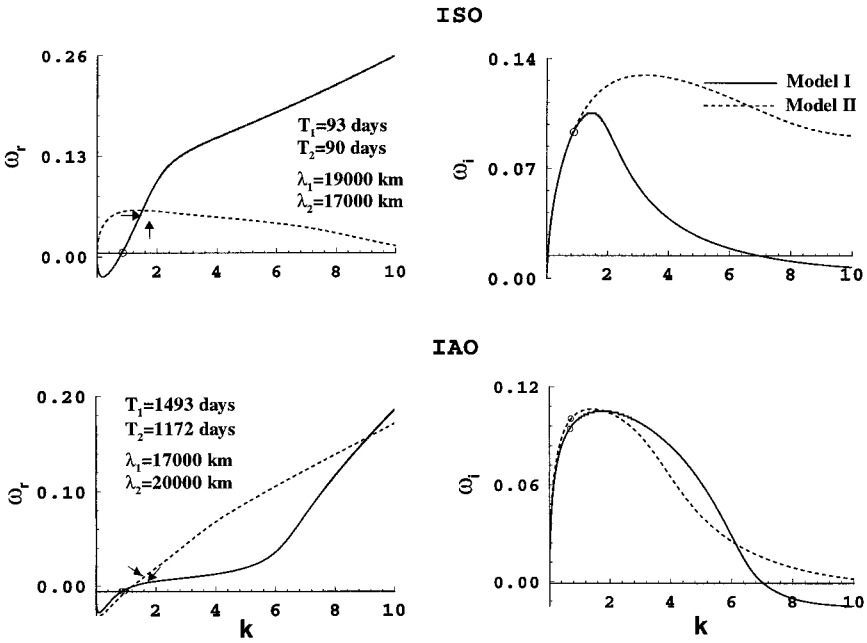

FIG. 1. Dispersion curves for the standard case (refer to Tables 1a and 1b). (left) The frequency (ω_r) as a function of wavenumber (k). (right) The corresponding growth rates (ω_i) as a function of k. (top) and (bottom) The intraseasonal and the interannual scenarios, respectively. The solid and the dashed lines represent, respectively, SST-model I and SST-model II. The allowed parts of the solutions are those starting from the circle marked at the smaller values of k. The arrow marks on the left panels indicate the wavenumbers corresponding to the SDW. The coordinates are in nondimensional units.

ranges of k. For IST (upper panels), the SDW for the ocean model I (solid line) belongs to this classical portion of the dispersion curve, while for the ocean model II the SDW has characteristics very different from those of an ordinary Kelvin wave. A similar observation also holds for the IAT (lower panels). Here the ocean model II has an SDW that resembles a classical Kelvin wave, while the SDW for the ocean model I (solid line) is very different from an ordinary Kelvin wave. This difference between the IAT and the IST is also reflected in the relations among the eigenfunctions.

The eigenfunctions for the maximally growing waves for the standard case are presented in Figs. 2–5. It can be seen that the eigenfunctions have very different correlations for the IAT and IST. The significance of this fact can be appreciated from a scrutiny of the energetics of the perturbations.

The bottom right panel in each figure shows the structure of the corresponding evaporation field. Once again, the correlations of the evaporation field with SST, moisture anomaly, and the zonal wind are different for different timescales and for the two SST models. The evaporation field is negatively correlated with SST and atmospheric temperature (T and θ, respectively) for the intraseasonal case for SST-model I and interannaul case for SST-model II (Figs. 2 and 5, respectively). This feature is also present for SST-model I in the case of IST scenario (Fig. 2). Such a feature in the observed field was reported by Cornejo-Garrido and Stone (1977), who found negative correlation between SST and evaporation and atmospheric heating in the regions of the Walker circulation near 10°S. Low correlation between SST and rainfall (s in our model) has been emphasized by also Ramage (1977). Murakami and Wang (1993) reported an out of phase relationship between OLR and SST from an investigation of annual cycle of the atmospheric circulation and SST over the equatorial Pacific and Indian Oceans. Due to lack of extensive observational analysis, it is not easy to verify these relations. There are, however, some evidence of such differences in the SST–evaporation correlations for different scenarios (Liu 1988).

f. Energetics

To gain further insight into the model behavior and elucidate the role of various physical mechanisms, analysis of the perturbation energetics is carried out. The total energy of the atmospheric and oceanic part are given by

$$\langle E_a \rangle_t = D_\theta^2 \frac{\eta_d \overline{q}}{\tau} \langle \theta s \rangle + D_s^2 \alpha_d \langle sT \rangle - \Lambda_d D_s^2 \langle s u_a \rangle, \quad (29)$$

where $E_a = (u_a^2 + D_\theta^2 \theta^2 + D_s^2 s^2)/2$ and $\eta_d = L_v/(C_p H \rho_a)$.

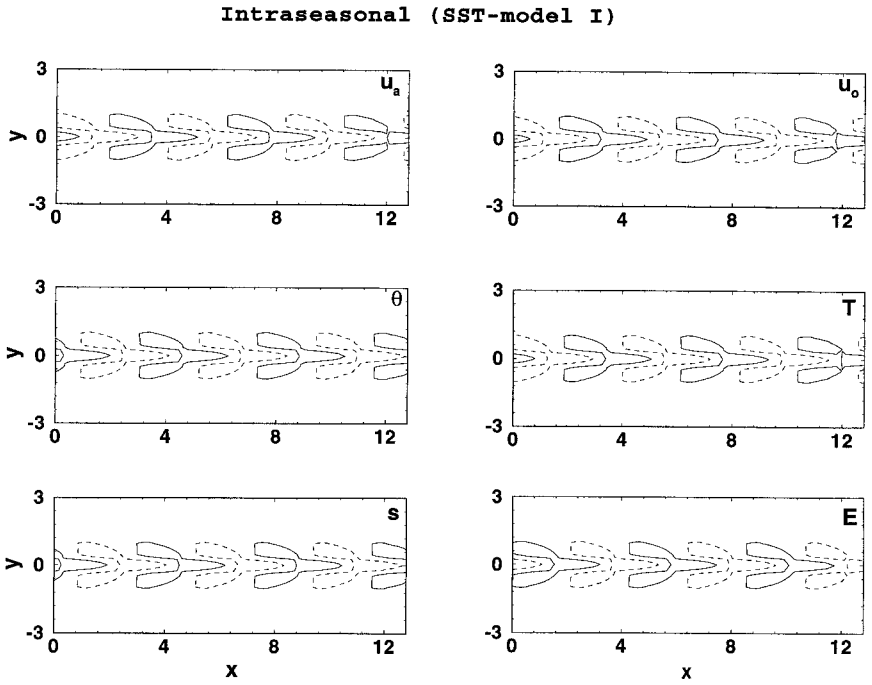

FIG. 2. Latitude–longitude plots of the atmospheric and oceanic eigenfunctions and the evaporation field (E) for the maximally growing wave for intraseasonal scenario for the ocean model I. The negative contours are dashed. The coordinates are in nondimensional units.

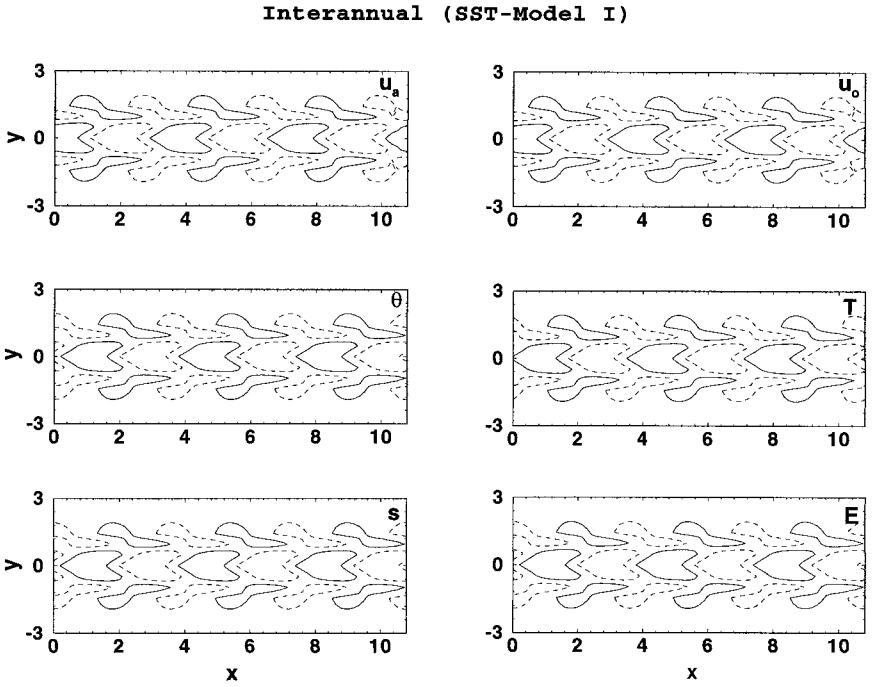

FIG. 3. Latitude–longitude plots of the atmospheric and oceanic eigenfunctions and the evaporation field (E) for the maximally growing wave for interannual scenario for the ocean model I. The negative contours are dashed. The coordinates are in nondimensional units.

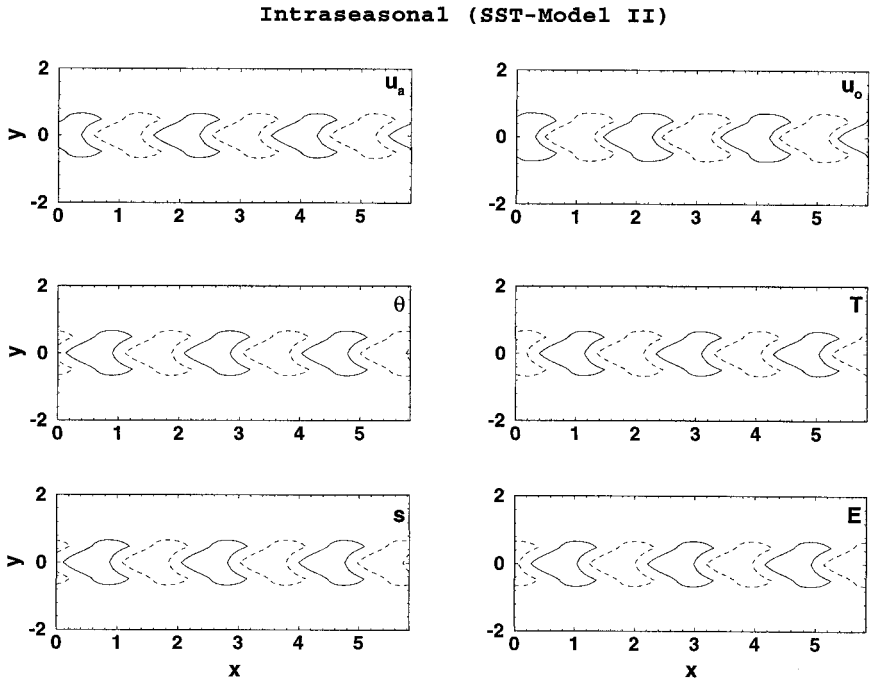

FIG. 4. Latitude–longitude plots of the atmospheric and oceanic eigenfunctions and evaporation field (E) for the maximally growing wave for intraseasonal scenario for the ocean model II. The negative contours are dashed. The coordinates are in nondimensional units.

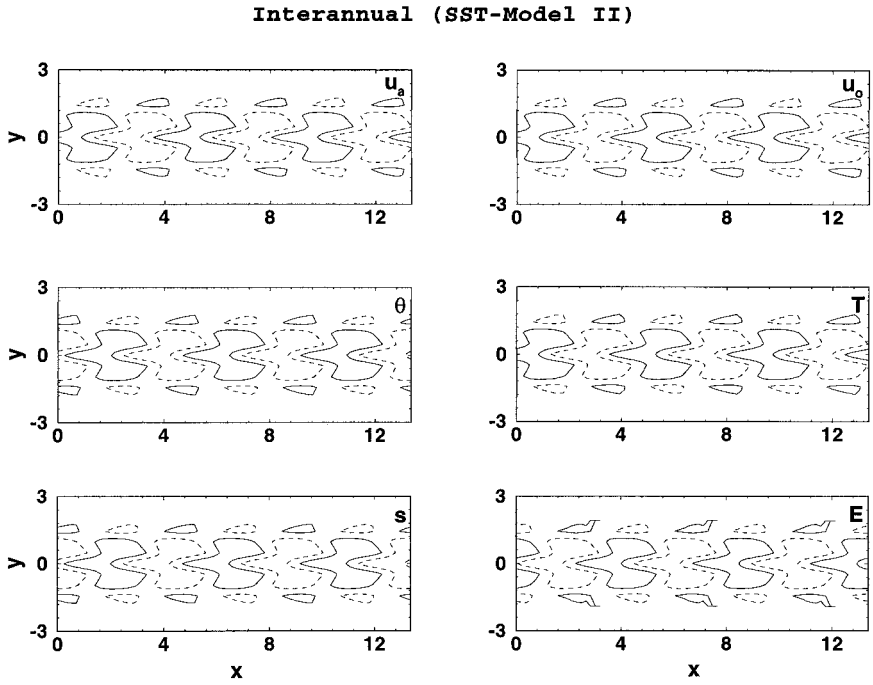

FIG. 5. Latitude–longitude plots of the atmospheric and oceanic eigenfunctions and the evaporation field (E) for the maximally growing wave for interannual scenario for the ocean model II. The negative contours are dashed. The coordinates are in nondimensional units.

TABLE 2a. Spectrum of convectively coupled oscillations (SST-model I).

Scenario					
	Parameters				
Timescales	Λ (10^{-1})	G (10^{-2})	Γ	T (day)	λ (10^3 km)
Intraseasonal	5.5	−12.5	1.35	107	18
	5.0	−10.5	1.35	93	19
Seasonal	5.0	−8.5	1.35	175	38
	4.0	−10.5	1.35	150	34
Annual	2.5	−10.5	1.10	331	10
	2.0	−8.5	1.10	337	10
Interannual	2.5	−8.5	1.00	1493	17
	2.0	−6.5	1.00	1527	1.6

TABLE 2b. Spectrum of convectively coupled oscillations (SST-model II).

Scenario					
	Parameters				
Timescales	Λ (10^{-1})	G (10^{-2})	Γ	T (day)	λ (10^3 km)
Intraseasonal	5.0	6.5	1.4	89	26
	6.5	8.5	1.4	98	34
Seasonal	3.0	−21	1.5	206	33
	3.0	−12.5	1.3	202	15
Annual	3.0	−8.5	1.3	336	20
	2.5	−10.5	1.3	386	27
Interannual	2.5	−5.0	1.2	2310	23
	2.5	−7.5	1.2	1172	20

SST-model I:

$$\langle E_o \rangle_t = \gamma_d \langle u_a u_o \rangle - D_h^2 \frac{d\overline{T}}{dx} \langle T u_0 \rangle, \qquad \overline{T} = \zeta \overline{h}, \quad (30)$$

where $E_O = (u_O^2 + D_T^2 T^2)/2$.

SST-model II:

$$\langle E_o \rangle_t = \gamma_d \langle u_a u_o \rangle - D_T^2 \frac{d\overline{T}}{dx} \langle T u_0 \rangle, \quad (31)$$

where $E_O = (u_O^2 + D_T^2 T^2 + \phi^2/g')/2$ with the angle bracket denotes average over a domain much larger than the disturbances. All D's in the above equations convert the dimension of the corresponding term into the dimension of energy. Exact forms of these conversion factors are not of much importance as we are interested in a qualitative study. The energy integrals of the oceanic equations show that, as found in earlier studies (Yamagata 1985), one of the necessary conditions for the instability is the net positive correlation between atmospheric wind and oceanic current. It can be seen from Fig. 2–5 that this condition is satisfied for both the models and scenarios. However, in the present case, this condition is neither necessary nor sufficient as evident from Eqs. (30)–(32). The correlation represented by $\langle Tu_o \rangle$ in the case of the IST scenario for model II is negative, which along with a positive SST gradient gives a positive contribution to the growth rate. This correlation is positive for model I for the IST scenario, which along with a $d\overline{T}/dx < 0$ gives a positive contribution. For the IAT, $d\overline{T}/dx$ for both the cases is negative, while corresponding $\langle Tu_o \rangle$ are generally positive, once again making the contribution positive. Another important source of energy, which is characteristic of convective coupling is $\langle su_a \rangle$, which is different for different scenarios. It also depends on the SST modeling to some extent. In the IST scenario, for model I, s and u_a are almost out of phase whereas for model II they are more in phase. For model II, the sign of Λ corresponding to IST scenario is negative. This implies a positive contribution to growth rate. This is also true for model I as the sign of Λ is positive. The term $\langle sT \rangle$, which measures the contribution to the growth rate from SST–evaporation feedback, is generally positive for both the scenarios and models.

4. Relative role of various processes

A large part of the variations in the characteristics of the oscillations at different timescales, we expect, is due to the variation in the strengths and the relative roles of various processes, represented by various model parameters. In view of the uncertainties involved in estimating many of these model parameters, it is important to address the question of sensitivity of our results to some of these parameters. As the number of parameters is rather large, we shall confine our study to those parameters that represent crucial physical processes. It, however, may not be consistent to investigate the variation of certain parameters alone over wide ranges. Since these parameters also represent certain mean conditions, their variations are likely to be accompanied by changes in certain other parameters. Hence, the characteristics of the SDW for different plausible combinations of these parameters are examined. Further, these sensitivity studies will be aimed at exploring certain specific issues of observed coupled variabilities in the Tropics.

The first question is how the spectrum of convectively coupled instabilities responds to a change in the scenario. Representative samples of the spectra of convectively coupled oscillations for the two ocean models are presented in Tables 2a and 2b, respectively, for different scenarios. It can be seen that for both the ocean models oscillations of appropriate period appear in a consistent manner as the scenario changes from one timescale to another. Table 2 also shows that while the characteristics of the SDW depend on the scenario parameters, the existence of coupled oscillation for a particular timescale is not critically dependent on the choice of these parameters.

The relative roles of various key processes in the excitation and the characteristics of the SDW are sum-

TABLE 3. Role of various processes in existence of selectively destabilized waves (for respective standard set values of other parameters).

	SST-Model I Scenario				SST-Model II Scenario			
	IST		IAT		IST		IAT	
Process	T (day)	λ (10^3 km)	T (day)	λ (10^3 km)	T (day)	λ (10^3 km)	T (day)	λ (10^3 km)
$\alpha = 0$	*		*		**		**	
$\Lambda = 0$	35	11	**		*		**	
$\Gamma = 0$	*		*		182	41	**	
$G = 0$	77	23	172	1.2	**		224	2.8
$\delta = 0$	Not applicable				91	2.6	4064	2.3

* Selection at the smallest scale.
** No growing modes.

marized in Table 3. It can be seen that there is no SDW in absence of OAC. The existence of an unstable mode (without scale selection) for $\alpha = 0$ is due to the fact that unlike in most linear analyses, the linear atmospheric component of our coupled model can by itself support unstable waves (GR). The important role played by east–west gradient of mean SST is also highlighted in this table.

a. Effect of mean westerlies

A well-known aspect of tropical circulation is the presence of strong surface westerlies over the monsoonal region due to the seasonal reversal of the winds. This reversal is also accompanied by a positive east–west gradient of SST over a large part of the Indian Ocean. It is important to investigate the effect of these changes in the mean conditions on the coupled oscillations at seasonal and intraseasonal timescales. Table 4 shows the characteristics of the SDW for the IST (and seasonal) scenario for mean westerlies ($\Lambda < 0$) and different strengths of the other scenario parameters G and Γ as well as for different strengths of α, while the other parameters are kept at their standard values. It can be seen from this table that coupled ISO appears only when mean westerlies are accompanied by a positive east–west gradient of mean SST. This is consistent with the fact that the monsoonal Indian Ocean is characterized by a positive gradient of mean SST. Another noteworthy feature is that SST-model I, which is more appropriate for the eastern Pacific region does not, in general, support modes of period less than seasonal timescale for mean westerlies, except for very high values of G. For SST model-II, on the other hand, the period of the SDW lies in the range of 30–110 days for a wide range of values of the scenario parameters. The corresponding wavelength also stays in the range of 15 000–24 000 km.

b. Interannual oscillations with short zonal scales

In order to explore whether a convectively coupled system can support interannual variabilities of different

TABLE 4. Effect of mean westerly on the selectively destabilized waves.

Parameters				SST-model I		SST-model II	
α	Λ (10^{-2})	Γ	G (10^{-1})	T (day)	λ (10^3 km)	T (day)	λ (10^3 km)
4.5	−11	1.1	1.25	212	15	94	24
4.5	−11	1.1	−1.25	**		**	
4.5	−11	1.1	12.5	47	22	39	19
4.5	−11	1.1	−12.5	*		**	
4.5	−11	1.2	1.25	356	10	90	17
4.5	−11	1.2	−1.25	**		**	
4.5	−11	1.2	12.5	48	16	38	15
4.5	−11	1.2	−12.5	*		**	
4.5	−22	1.2	1.25	*		111	18
4.5	−22	1.2	−1.25	**		**	
4.5	−22	1.2	12.5	57	16	43	15
4.5	−22	1.2	−12.5	*		**	
9.0	−11	1.2	1.25	226	8.0	68	16
9.0	−11	1.2	−1.25	**		**	
9.0	−11	1.2	12.5	35	15	30	15
9.0	−11	1.2	−12.5	*		**	

* Selection at smallest scale.
** Growing mode absent.

TABLE 5. IAO with short zonal scale (SST-Model II).

Parameters				
α	Λ (10^{-1})	G (10^{-2})	T (day)	λ (10^3 km)
9.5	−6.5	8.5	1201	8.7
4.5	−5.0	8.5	1336	9.1
12.5	−6.5	6.5	1827	8.7
4.5	3.5	5.0	1141	8.1
9	5	8.0	1985	7.1

TABLE 7. Effect of mean wind strength and broad spectrum ISO.

		SST-Model I*		SST-Model II**	
$\bar{u}$ (m s^{-1})	γ (10^{-3})	T (day)	λ (10^3 km)	T (day)	λ (10^3 km)
10	19.0	44	11	69	16
7	13.5	65	13	79	16
5	9.60	87	15	90	17

* $\Lambda = 0.65$, $\Gamma = 1.3$, $G = 0.12$.
** $\Lambda = -0.13$, $\Gamma = 1.3$, $G = 0.12$.

zonal scales as observed, we have considered a number of scenarios for the interannual scale. The results are presented in Table 5. It is interesting to note that while the SST-model II can give rise to IAO with relatively short zonal scales for a number of scenarios, such a trend is not available for SST-model I. As emphasized earlier, the SST-model II, which does not assume a shallow thermocline as in SST-model I is more appropriate for the Indian Ocean region. For SST-model II, interannual modes with period ranging from about 3 to 5 yr appear for a very wide range of parameters. A comparison of Tables 2b and 5 reveals that EWF and zonal gradient of mean SST are two primary mechanisms that give rise to these IAO with short zonal scales. The importance of role of EWF in the IAO over the Indian Ocean has been recently emphasized by Goswami and Harinath (1997).

c. Role of convective time lag

While the above investigations provide an extensive study of sensitivity of the results to the model parameters, we present below a summary of a conventional sensitivity study of the existence and the characteristics of the SDW with respect to certain model parameters. Of particular importance is the sensitivity of the results to the value of CTL. All of the above studies were done for a fixed value (0.25 day) of CTL. It is also one of the parameters that cannot be assigned a precise value since it embodies our hypothesis of CTL. As argued in GR, its value should be a few hours. It is, however, desirable that the existence and characteristics of the SDW for the two SST models and for different scenarios do not depend sensitively on the value of τ. The values of period and wavelength of the SDW for the two scenarios and for the two SST models are presented in Table 6 for a range of CTL. We note that our results do not depend critically on the value of τ. Indeed, for a fourfold change in the value of τ, from 0.1 to 0.4 day, the time periods for the SDW for the IST scenario remain within 66 and 115 days for SST-model I and between 95 and 83 days for SST-model II. The corresponding wavelengths are between 15 000 and 28 000 km. For the IAT scenario, the time periods of the SDW for the SST-model II are between 1144 and 1280 days, with corresponding wavelengths between 15 000 and 22 000 km. For SST-model I, however, the changes in the time period are much larger, from 663 days to 2308 days. Also, the trends of change in the time period as well as wavelength in the case of the SST-model II for IAT scenario are opposite to those for other cases. Although the reasons for this are not clear, it was found that the solutions of the dispersion relations enter different regimes depending upon the relative strengths of the parameters.

d. Effect of mechanical coupling and broad spectrum ISO

Since the strength of the mechanical coupling (γ) is controlled by the strength of the mean wind, it is likely to have different strengths for different timescales or for different situations. The sensitivity of the coupled oscillations to the strength of the mechanical coupling [or, equivalently, the product $\alpha\gamma$, since α and γ always appear together in Eqs. (18) and (19)] is shown in Table 7. The values of the mean winds corresponding to these values of γ are also given in the table. We assume that the strongest value of γ represents, qualitatively, the IST

TABLE 6. Effect of convective time lag on characteristics of the maximally growing waves.

Convective time lag		SST-Model I Scenario				SST-Model II Scenario			
		IST		IAT		IST		IAT	
τ (day)	$B = \frac{T_0}{\tau}$	T (day)	λ (10^3 km)	T (day)	λ (10^3 km)	T (day)	λ (10^3 km)	T (day)	λ (10^3 km)
0.1	8.5	115	21	663	15	95	28	1280	22
0.2	4.2	101	20	1093	16	91	26	1253	21
0.3	2.8	85	18	2271	17	88	25	1158	18
0.4	2.0	66	15	2302	18	83	24	1144	15

TABLE 8. Sensitivity of characteristics of SDW to scenario parameters (IST).

Parameter		SST-Model I		SST-Model II	
Symbol	Value	T (day)	λ (10^3 km)	T (day)	λ (10^3 km)
Λ (10^{-1})	2.5	29	16	*	*
	3.5	53	16	*	*
	4.5	87	18	82	24
	5.5	104	19	101	29
	6.5	115	20	116	35
Γ	1.0	316	12	113	23
	1.1	106	6.7	103	22
	1.2	54	2.9	96	22
	1.3	71	15	93	24
	1.4	109	22	90	25
	1.5	125	27	87	27
G (10^{-2})	−2.0	82	22	165	30
	−4.0	87	21	114	27
	−6.0	92	20	90	26
	−8.5	93	19	73	24
	−10	93	18	62	22
	−12	94	18	52	20

* Selection at smallest scale.

TABLE 9. Sensitivity of characteristics of SDW to scenario parameters (IAT).

Parameter		SST-Model I		SST-Model II	
Symbol	Value	T (day)	λ (10^3 km)	T (day)	λ (10^3 km)
Λ (10^{-1})	1.5	**		320	16
	2.5	2221	17	3655	24
	3.5	366	14	*	
	4.5	223	12	*	
	5.5	170	11	*	
Γ	1.0	2986	18	*	
	1.1	192	8.0	*	
	1.2	*		1100	30
	1.3	*		893	40
	1.4	*		673	48
G (10^{-2})	−6.7	537	15	1394	20
	−7.1	634	15	1289	20
	−7.5	779	16	1132	19
	−7.9	1028	16	1009	18
	−8.3	1493	17	910	18

* Selection at smallest scale.
** Growing mode absent.

scenario, with strong mean wind. It can be seen that as the strength of the mean wind (coupling) is decreased from 10 m s^{-1} ($\gamma = 19$) to 5 m s^{-1} ($\gamma = 9.6$), the period of the coupled ISO increases, from 44 days to 87 days for SST-model I, and from 69 days to 90 days for SST-model II. The corresponding changes in the wavelengths are, however, marginal, especially for the SST-model I. It is interesting to note that in an analysis of SST data for the period 1979–85, E87 had recorded eastward propagating oscillations with period 40–60 days, while MT, in their analysis for the period 1983–86 for the same region recorded Kelvin wave–like disturbances of period 60–90 days. As observed by MT, this could be due to the changes in the variables due to the El Niño of 1982–83. Indeed, the analysis of E87 shows that subsequent to the El Niño the period increased to 70 days. MT concludes that the two oscillations observed by E87 and MT are essentially the same phenomenon. Table 7 provides a qualitative support for such a broad spectrum ISO due to changes in the mean conditions, although, in practice, more than one mean process (such as zonal gradient of mean SST) is likely to be involved.

e. Effect of EWF, mean SST gradient, and Γ

As we have emphasized earlier, an arbitrary and independent variation of parameters like Λ and G is not justified as such a variation would imply a change in certain mean conditions and hence corresponding changes in the other scenario parameters. However, for the sake of completeness, we present in Tables 8 and 9 variations in the characteristics of the SDW for both the ocean basins with respect to Λ, G, and Γ, for the IST and IAT, respectively. In each of these cases only one parameter was varied when all other parameters were kept constant (at their standard values). As we have seen in Table 3, the existence of SDW critically depends on the processes of evaporation–SST feedback (α) and EWF. There is no SDW for $\alpha = 0$, while there is SDW only at ISO for $\Lambda = 0$ (Table 3). Further, as discussed in the context of interannual and intraseasonal scenarios, Λ significantly affects the characteristics of the SDW. This trend is further reflected in Tables 8 and 9. For both the scenarios, Λ has a profound effect on the existence and the nature of the SDW. The sensitivity of existence of SDW on Λ, however, is more sensitively dependent in the case IAT (Table 9), especially for SST-model II. The existence of IAO is also sensitive to Γ, as can be seen from Table 9. The characteristics of IAO are, relatively, less sensitive to variations in G.

A scrutiny of Tables 8 and 9 reveals that the existence of SDW with ISO characteristics is supported by a much wider range of scenario parameters in the intraseasonal scale than in the interannual scenario. However, as we have mentioned earlier, conclusions from such independent variation of the scenario parameters may have only limited validity.

5. Discussions and conclusions

The emphasis of the present work has been on a unified dynamical framework for the genesis of a wide class of tropical variabilities. In our scenario, there is a basic dynamical mechanism that, under the interplay of various processes involved, gives rise to selective excitations at a number of observed spatial and temporal

scales. The detailed structures of these observed oscillations, of course, will be enriched by various other processes, including nonlinear processes, that operate beyond the genesis of the waves.

The dynamical mechanism is that of selective excitation of tropical Kelvin wave at various scales through internal forcing generated by OAC and moist processes. The motivation for exploring Kelvin waves has come from the predominantly Kelvin wave character of many observed tropical variabilities. The two distinguishing features of the present framework is an explicit dynamics of the moisture variable controlled by a convective time lag, and a convective OAC. The inclusion of an explicit moisture equation implies that we do not restrict our system to be necessarily in a *convective regime* assumed in many earlier studies (Goswami and Selvarajan 1991; LS). The inclusion of CTL embodies the hypothesis that the selective destabilization (or high-frequency cutoff) takes place through forcing by convection organized at certain timescales (characterized by CTL). The basic premise of convective coupling is that the atmosphere does not respond directly to SST heat source, but only through deep column heating associated with precipitation. OAC controls this precipitational heating through the effect of SST on column moisture. However, as precipitation is a threshold process, convective coupling makes OAC also a (second order) threshold process. Although more complex coupled dynamics have been considered with conventional direct coupling (Hirst 1986; Hirst and Lau 1990), the present study stands apart from these earlier studies for its emphasis on convective OAC as a genesis mechanism for a wide spectrum of waves with observed spectral characteristics. It is also worth mentioning that our moisture dynamics [Eqs. (4) and (6)] does not collapse to the more widely used scenario where precipitation is determined by a balance between column convergence and surface evaporation. One way to see this is that putting $\partial s/\partial t = 0$ in Eq. (4) removes the moisture variable from the basic dynamics and Eq. (6) for precipitation becomes indeterminate. Similarly, the situation with $\tau = 0$ has to be separately formulated as conceptually and mathematically $\tau = 0$ results in an infinite rate of precipitation and hence infinite rate of heating.

One of the chief merits of the convective coupling is that it naturally supports coupled modes at a number of timescales, which correspond to the spectrum of observed variabilities. The same mechanism that excites the intraseasonal mode for the IST scenario selectively excites the interannual mode when the scenario changes to IAT, as characterized by the relative strengths of the processes. In our analysis, these different variabilities emerge as SDW of time and length scales governed by the mean conditions. Further, these variabilities can coexist with their respective characteristics as in nature, as they respond to different mean conditions. Indeed, for the IST scenario, only rarely is an IAO signal excited and vice versa. Another interesting fact is that while the periods of SDW change with scenario parameters, these changes are in discrete and separated bands, such as intraseasonal, seasonal, and interannual, as we change the parameter regimes. It is also worth mentioning that the range of variations of various model parameters in our sensitivity studies is much larger than the uncertainties in the estimation of these parameters. The actual variations of the spectral characteristics of the SDW in a particular case are, therefore, going to be smaller. On the other hand, spatial variations of these parameters offer a qualitative but natural explanation for the spatial variations in the characteristics of the observed variabilities.

The present formalism also supports interannual oscillation with relatively small zonal scale when the SST dynamics corresponds to a situation with a deep thermocline. Such a framework may have relevance in the genesis of interannual oscillations over the Indian Ocean almost in phase with ENSO, as shown by recent observational analysis. Since the IAO with shorter zonal scales can coexist with interannual oscillations of comparable periods but larger zonal scales in an ocean basin with different SST dynamics, like the ENSO with larger zonal scale over the Pacific, the present formalism offers a unified dynamical framework for genesis of coupled IAO in the global Tropics.

While the appearance of a SDW at a number of observed spatial and temporal scales is encouraging, it must be emphasized that the scope of the present work is limited to the genesis of these variabilities. The observed dynamics of these variabilities will be necessarily richer than a pure Kelvin wave as there will also be other processes that will come into play once the wave is excited. The associated Rossby wave in case of ENSO could be such an example. Similarly, location-specific processes and factors, like SST–thermocline feedback and different mean gradients will also become important. Another limitation of the present model is that it provides a comparison of only certain observed properties (such as wavelength and time period). It does not allow a comparison of the detailed observed dynamics. It is for this reason that we do not directly identify the detailed (i.e., except spectral characteristics) structure of the observed variabilities with those of the SDW. These limitations, along with the absence of nonlinearities and multiple ocean basins must be kept in view while interpreting the results.

In spite of its simplicity and the limitations inherent in a linear setting, the present results, we feel, provide valuable insight into the relevance and effect of convective coupling in the dynamics of tropical oscillations. The appearance of SDW at a number of observed spatio-temporal scales, with various other (qualitative) correspondence with observations, is unlikely to be a mere coincidence. It is also noteworthy that convectively coupled Kelvin waves may exhibit structures (eigen functions) quite different from the conventional one, as shown in Figs. 3 and 5. Inclusion of COAC in models

of climate, therefore, may significantly improve the simulation of tropical variabilities, thereby improving the quality and range of forecast. In particular, the present study indicates that OAC may play a significant role also in subseasonal range forecast. To overcome some of the shortcomings of the present model and take it to its logical conclusion, the next step must be to incorporate COAC in a (numerical) model, which allows the inclusion of observed basin geometry, more elaborate dynamics (such as inclusion of other modes), as well as essential nonlinear processes. Comparison of simulated climatology from such a model with observed climatology can then indirectly verify the validity and the relevance of convective coupling.

Acknowledgments. The authors would like to thank anonymous referees for comments that led to certain corrections in the manuscript. This study was partly supported by a Research Grant from ONR.

REFERENCES

Barnett, T. P., 1984: Interaction of monsoon and pacific trade wind system at interannual time scales. Part III: A partial anomaly of Southern Oscillation. *Mon. Wea. Rev.,* **112,** 2380–2387.

Betts, A. K., 1986: A new convective adjustment scheme. Part I: Observational and theoretical basis. *Quart. J. Roy. Meteor. Soc.*, **112,** 677–691.

——, and M. J. Miller, 1986: A new convective adjustment scheme. Part II: Single column tests using GATE wave, BOMEX, ATEX and Artic air-mass data sets. *Quart. J. Roy. Meteor. Soc.,* **112,** 693–709.

Bjerknes, J., 1969: Atmospheric teleconnections from the equatorial Pacific. *Mon. Wea. Rev.,* **97,** 163–172.

Cornejo-Garrido, A. G., and P. H. Stone, 1977: On the heat balance of the Walker circulation. *J. Atmos. Sci.,* **34,** 1155–1162.

Davey, M. K., 1985: Result from the moist equatorial atmosphere model, *Coupled Ocean–Atmosphere Models,* J. C. J. Nihoul, Ed., Elsevier, 41–49.

——, and A. E. Gill, 1987: Experiment on tropical circulation with a simple moist model. *Quart. J. Roy. Meteor. Soc.,* **113,** 1237–1269.

Emanuel, K. A., 1993: The effect of convective response time on WISHE modes. *J. Atmos. Sci.,* **50,** 1763–1775.

Enfield, D. B., 1987: The intraseasonal oscillation in eastern Pacific sea levels: How is it forced? *J. Phys. Oceanogr.,* **17,** 1860–1876.

Goswami, B. N., and S. Selvarajan, 1991: Convergence feedback and unstable low frequency oscillation in a simple coupled ocean–atmospheric model. *Geophys. Res. Lett.,* **18,** 991–994.

Goswami, P., and B. N. Goswami, 1991: Modification of $n=0$ equatorial waves due to interaction between convection and dynamics. *J. Atmos. Sci.,* **48,** 2231–2244.

——, and R. Koteswar Rao, 1994: A dynamical mechanism for selective excitation of the Kelvin mode at timescale of 30–50 days. *J. Atmos. Sci.,* **51,** 2769–2779.

——, and V. Mathew, 1994: A mechanism for scale selection in tropical circulation at observed intraseasonal frequencies. *J. Atmos. Sci.,* **51,** 3155–3166.

——, and N. Harinath, 1997: A mechanism for observed interannual variablities over the equatorial Indian Ocean. *J. Atmos. Sci.,* **54,** 1689–1700.

Hendon, H., and J. Glick, 1995: Observed intraseasonal atmosphere–ocean variability in the tropical Pacific and Indian Oceans. *Abstract, Int. Scientific Conf. on Tropical Oceans Global Atmosphere,* Melbourne, Australia.

Hirst, A. C., 1986: Unstable and damped equatorial modes in simple coupled ocean–atmospheric models. *J. Atmos. Sci.,* **43,** 606–630.

——, 1988: Slow instabilities in tropical ocean basin–global atmosphere models. *J. Atmos. Sci.,* **45,** 830–852.

——, and K. M. Lau, 1990: Intraseasonal and interannual oscillations in coupled ocean–atmosphere models. *J. Climate,* **3,** 713–725.

Johnson, E. S., and M. J. McPhaden, 1993: Structure of intraseasonal Kelvin waves in the equatorial Pacific Ocean. *J. Phys. Oceanogr.,* **23,** 608–625.

Jones, C., and B. C. Weare, 1996: The role of low-level moisture convergence and oceanic latent heat fluxes in the Madden–Julian oscillation: An observational analysis using ISCCP data and ECMWF analyses. *J. Climate,* **9,** 3086–3104.

Knutson, T., and K. M. Weickmann, 1987: The 30–60 day atmospheric oscillations: Composite life cycles of convection and circulation anomalies. *Mon. Wea. Rev.,* **115,** 1407–1436.

Lau, K. M., and P. H. Chan, 1985: Aspect of 40–50 day oscillation during northern winter as inferred from outgoing long wave radiation. *Mon. Wea. Rev.,* **113,** 1889–1901.

——, and S. Shen, 1988: On the dynamics of the intraseasonal oscillation and ENSO. *J. Atmos. Sci.,* **45,** 1781–1797.

Lau, N. C., and K. M. Lau, 1986: Structure and propagation of intraseasonal oscillations appearing in a GFDL GCM. *J. Atmos. Sci.,* **43,** 2023–2047.

Liu, W. T., 1988: Moisture and latent heat flux variabilities in the tropical Pacific derived from satellite data. *J. Geophys. Res.,* **93,** 6749–6760.

Madden, R. A., and P. R. Julian, 1971: Detection of a 40–50 day oscillation in the zonal wind in the tropical pacific. *J. Atmos. Sci.,* **28,** 702–708.

——, and ——, 1972: Description of global scale circulation cells in the tropics with a 40–50 day period. *J. Atmos. Sci.,* **29,** 1109–1123.

Mayers, G., J. R. Donguy, and R. K. Reed, 1986: Evaporative cooling of western equatorial Pacific Ocean by anomalous winds. *Nature,* **323,** 523–526.

McPhaden, M. J., and B. A. Taft, 1988: Dynamics of seasonal and intraseasonal variability in the eastern Pacific. *J. Phys. Oceanogr.,* **18,** 1713–1732.

Mitchell, T. P., and J. M. Wallace, 1992: The annual cycle in equatorial convection and sea surface temperature. *J. Climate,* **5,** 1140–1156.

Murakami, T., and B. Wang, 1993: Annual cycle of equatorial east–west circulation over the Indian and Pacific Oceans. *J. Climate,* **6,** 932–952.

Neelin, J. D., and J.-Y. Yu, 1994: Modes tropical variability under convective adjustment and Madden–Julian oscillation. Part I: Analytical theory. *J. Atmos. Sci.,* **51,** 1876–1914.

——, I. M. Held, and K. H. Cook, 1987: Evaporation–wind feedback and low frequency variability in tropical atmosphere. *J. Atmos. Sci.,* **43,** 2341–2348.

Nigam, S., and H. S. Shen, 1993: Structure of oceanic and atmospheric low frequency variabilities over the tropical Pacific and Indian Oceans. Part 1: COADS observation. *J. Climate,* **6,** 657–677.

Philander, S. G., 1990: *El Niño, La Niña, and Southern Oscillation.* Academic Press, 293 pp.

——, T. Yamagata, and R. C. Paicanowski, 1984: Unstable air–sea interaction in the Tropics. *J. Atmos. Sci.,* **41,** 604–613.

Ramage, C. S., 1977: Sea surface temperature and local weather. *Mon. Wea. Rev.,* **105,** 540–544.

Rasmusson, E. M., X. Wang, and C. F. Repelowski, 1990: Biennial component of ENSO variability. *J. Mar. Syst.,* **1,** 71–96.

Seager, R., and S. E. Zebiak, 1995: Simulation of tropical climate with a linear primitive equation model. *J. Climate,* **8,** 2497–2520.

Shinoda, T., H. H. Hendon, and J. Glick, 1998: Intraseasonal variability of surface fluxes and sea surface temperature in the tropical western Pacific and Indian Oceans. *J. Climate,* **11,** 1685–1701.

Toure, Y. M. and W. B. White, 1995: ENSO signals in global upper

ocean temperature. *Abstracts, Int. Scientific Conf. on Tropical Oceans Global Atmosphere,* Melbourne, Australia, 119.

Wang, X. L., 1994: The coupling of annual cycle and ENSO over the tropical Pacific. *J. Atmos. Sci.,* **51,** 1115–1138.

Weare, B. C., 1994: Interrelationships between cloud properties and sea surface temperature on seasonal and interannual time scales. *J. Climate,* **7,** 248–260.

——, P. T. Strub, and D. Michel, 1981: Annual mean surface heat fluxes in the tropical Pacific Ocean. *J. Phys. Oceanogr.,* **11,** 705–717.

Weickman, K. M., G. R. Lussky, and J. E. Kutzbach, 1985: Intraseasonal (30–50 day) fluctuations in outgoing longwave radiation and 250 mb streamfunction during northern winter. *Mon. Wea. Rev.,* **113,** 941–961.

Yamagata, T., 1985: Stability of simple air–sea coupled model in the Tropics. *Coupled Ocean-Atmosphere Models,* J. C. J. Nihoul, Ed., Elsevier, 637–657

Yasunari, T., 1987: Global structure of El Niño Southern Oscillation. Part 1: El Niño composites. *J. Meteor. Soc. Japan,* **65,** 65–68.

Zebiak, S. E., 1993: Air–sea interaction in the equatorial Atlantic region. *J. Climate,* **6,** 1567–1586.

Zhang, G. J., and M. J. MacPhaden, 1995: The relationship between sea surface temperature and latent heat flux in the equatorial Pacific. *J. Climate,* **8,** 589–605.